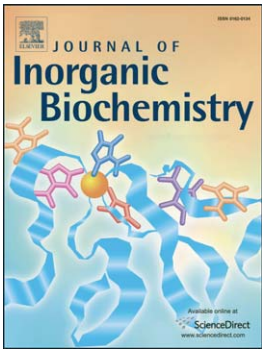

Synthesis, characterization and anti-diabetic therapeutic potential of novel aminophenol-derivatized nitrilotriacetic acid vanadyl complexes

Na Wang, Ziwei Wang, Xia Niu, Xiaoda Yang

PII: S0162-0134(15)30040-4
DOI: doi: 10.1016/j.jinorgbio.2015.07.012
Reference: JIB 9765

To appear in: *Journal of Inorganic Biochemistry*

Received date: 28 March 2015
Revised date: 3 July 2015
Accepted date: 15 July 2015

Please cite this article as: Na Wang, Ziwei Wang, Xia Niu, Xiaoda Yang, Synthesis, characterization and anti-diabetic therapeutic potential of novel aminophenol-derivatized nitrilotriacetic acid vanadyl complexes, *Journal of Inorganic Biochemistry* (2015), doi: 10.1016/j.jinorgbio.2015.07.012

Synthesis, characterization and anti-diabetic therapeutic potential of novel aminophenol-derivatized nitrilotriacetic acid vanadyl complexes

Na Wang, Ziwei Wang, Xia Niu, and Xiaoda Yang*

State Key Laboratories of Natural and Biomimetic Drugs and Department of Chemical Biology, School of Pharmaceutical Sciences, Peking University Health Science Center, Beijing 100191, P. R. China

* Corresponding author: Xiaoda Yang

Fax: +86-10-82805611, E-mail: xyang@bjmu.edu.cn.

ABSTRACT

In the present work, we synthesised three novel aminophenol-derivatized nitrilotriacetic acid vanadyl complexes (VOohpada,VOmhpada,VOphpada) using the strategy of rational incorporation of antioxidant groups in ligand in order to balance the side effects with the therapeutic properties. The complexes were characterized by IR, UV-VIS, ESI-MS and elemental analysis. The biological evaluations in *vitro* revealed that the position of the hydroxyl group of aminophenol moiety regulated the antioxidant activity of the complexes as well as the cytotoxicity on HK-2 cells. The vanadyl complex of *p*-hydroxyl aminophenol derivative (VOphpada) exhibited better antioxidant activity and lower cytotoxicity than other analogs. In type II diabetic *db*/*db* mice, VOphpada (0.1 mmol/kg/day) effectively reduced blood glucose level, improved glucose tolerance, and alleviated stresses induced by hyperglycemia and hyperlipidemia. VOphpada treatment significantly increased expression of PPARα and γ, activated Akt, and inactivated JNK in muscle and adipose tissues. The insulin enhancement effects of VOphpada were observed more potent than BMOV. Moreover, VOphpada decreased the level of kidney injury molecule-1 marker (KIM-1), suggesting a potentially lower renal toxicity. In overall, the present results suggest VOphpada as a novel hypoglycemic agent with improved efficacy-over-toxicity index.

Key words: vanadium; diabetes; aminophenol; PPARα; PPARγ

1. Introduction

Vanadium compounds are promising anti-diabetic agents [1, 2]. In previous efforts to improve pharmacokinetic properties and eliminate gastrointestinal stress, a great deal of vanadium complexes with organic ligands have been synthesized and evaluated for their insulin mimetic activity, e.g. bis(maltolato)oxovanadium (BMOV) and its ethyl analog BEOV by Orvig et al. [1, 3], bis(allixinato)-oxovanadium(IV) and bis(picolinato)oxovanadium(IV) by Sakurai et al. [4-7] and vanadium (III, IV, V)-dipicolinate by Crans et al. [8-10]. Since the failure of BEOV in phase II clinical trial due to renal side effect [11], a great challenge has emerged as how to modulate vanadium metal toxicity to develop novel vanadium complexes with good balance between the therapeutic properties and the side effects [2, 12].

Although the mechanism of the renal toxicity of BMOV/BEOV has not been elucidated, many studies have suggested that vanadium-induced oxidative stress due to interaction with mitochondria could be one major mechanism for vanadium toxicity [13, 14]. In addition, vanadium-induced inflammatory responses could also be involved [15], amongst which induction of cyclooxygenase-1,2 (COX-1,2) has been proposed as the main source of pro-inflammatory factors upon vanadium treatment [16, 17].

Natural and synthetic antioxidants were shown to effectively decrease vanadium toxicity [18-20]. Therefore, incorporation of antioxidant groups in the structure of vanadium complexes could be a feasible strategy in designing novel anti-diabetic vanadium complexes with lower toxicity. Flavonoids are excellent natural occurring antioxidants. A series of vanadyl flavonoid complexes [21-30] have been synthesized. These complexes were shown to

be non-toxic and reverse metabolic changes in diabetic mice [22, 23]. Using a different strategy, we prepared a salicylic acid-derivatized kojic acid vanadyl complexes (BSOV) [31, 32]. BSOV exhibited a similar effect in reducing the blood glucose level and a lower acute toxicity associated with the higher antioxidant activity [31] .

In the present paper, we report the synthesis and evaluation of novel aminophenol-derivatized nitrilotriacetic acid vanadyl complexes. In design of the ligand, nitrilotriacetate was chosen as the metal binding moiety in order to reduce molecular size and improve the solubility of the complexes. The moiety of acetylaminophenol, a specific inhibitor of COX-1, 2, and 3 [33] , was incorporated in the ligand in order to provide antioxidative and anti-inflammatory activity. The experimental results showed that the vanadyl complex of *p*-aminophenol derivative showed improved therapeutic potency over BMOV.

2. Experimental section

2.1. *Materials and Instrumentation*

Vanadyl sulfate ($VOSO_4 \bullet xH_2O$, x=3 to 5) was purchased from Sigma-Aldrich (St. Louis, MO, USA), Vanadyl acetylacetonate ($VO(acac)_2$) was from Fluka (Steinheim, Germany). Antibodies for PPARγ, AKT, phosphorylated JNK (p-JNK) and GAPDH were from Santa Cruz Biotechnology (Santa Cruz, CA, USA). Antibodies for PPARα were from Cell Signaling Technology (Cell Signaling Technology, Inc. Beverly, MA, US). BSA (fraction V) and 3-(4,5-dimethylthiazoyl-2-yl)-2,5-diphenyltetrazolium bromide (MTT) were from Sigma-Aldrich (Milwaukee, WI, USA). L-Ascorbic acid was from Beijing Chemical Reagent

Company (Beijing, China). All other chemicals and solvents were reagent grade and used without further purification unless otherwise specified. Bis(maltolato)oxovanadium (BMOV) was prepared and purified according to the published method [34].

The synthesized ligands and their complexes were characterized by infrared (IR) spectroscopy, UV-VIS spectroscopy, mass spectrometry, elemental analysis, and NMR spectroscopy. Where appropriate, ^{1}H NMR was used for further characterization. Infrared spectra were recorded as KBr disks in the range 4000–400cm^{-1} on a Nexus-470 FTIR spectrophotometer (Nicolet Instruments, USA). UV-VIS spectra were performed on a Techcomp 3100 spectrophotometer (Techcomp Ld., China). Mass spectra (Negative ion mode) were obtained with a QSTAR quadrupole time-of-flight (TOF) hybrid mass spectrometer (Applied Biosystems, USA).

2.2. *Synthesis*

The synthesis route is illustrated in Scheme 1:

[Scheme 1]

Nitrilotriacetic anhydride (**2**). Compound 2 was prepared according to a previously reported method [35].

N-(hydroxyphenylcarbamoylmethyl) iminodiacetic acid (H_2hpada)(**3a,b,c**). Under the protection of nitrogen, compound 2 (20 mmol) and (*p*,*o*,*m*-)aminophenol (20 mmol) were dissolved into 50 mL of N,N-dimethylformamide (DMF). After stirring for 10 min, 6 mL of pyridine was added. The mixture was heated with stirring for 24 h in an oil bath at 70 °C. Then the solvent was evaporated under reduced pressure. The residue was dissolved in 100

mL water, and the solution was adjusted to pH 9.18 with 2 M sodium hydroxide solution and extracted with ethyl acetate. The water phase was then adjusted to pH 2.85 with 6 M hydrochloride. The crude product was collected by filtration and further purified by recrystallization in DMF.

3a (*p*-H_2hpaida):White; Yield 60.75%; IR (cm^{-1}): 3309 cm^{-1}($V_{(O-H)}$); 1580 cm^{-1},1399 cm^{-1}, 808 cm^{-1} (ring $V_{C=C}$);1661 cm^{-1} ($Vas_{(COO)}$);1355 cm^{-1} ($Vs_{(COO)}$); ^{1}H NMR (δ):10.02 (s,1H);7.39-7.41 (d,J = 7.2 Hz,2H); 6.70-6.72 (d,J = 7.2Hz,2H); 3.53 (s,4H); 3.44 (s,2H); ESI-MS:*m/z* 281 $[M-1]^-$, MW calc. ($C_{12}H_{14}O_6N_2$) 282.25.

3b (*m*-H_2hpada): light yellow; Yield 61.49%; IR (cm^{-1}):3433 cm^{-1} ($V_{(O-H)}$); 1600 cm^{-1} ,1489 cm^{-1} (ring $V_{C=C}$); 1637 cm^{-1} ($Vas_{(COO)}$); 1417 cm^{-1} ($Vs_{(COO)}$); ^{1}H NMR (δ): 10.13 (s,1H); 7.23 (s,1H); 7.08 (t, J = 8.0Hz,1H); 6.95 (d, J =8.0Hz,1H); 6.47 (d,J = 8.5Hz,1H); 3.54 (s,4H); 3.45 (s,2H); ESI-MS: *m/z* 281 $[M-1]^-$, MW calc. ($C_{12}H_{14}O_6N_2$) 282.25.

3c (*o*-H_2hpada): White; Yield 64.72%; IR (cm^{-1}): 3346 cm^{-1} ($V_{(O-H)}$);1617 cm^{-1},1502 cm^{-1}, 814 cm^{-1},747 cm^{-1} (ring $V_{C=C}$); 1659 cm^{-1} ($Vas_{(COO)}$); 1468 cm^{-1} ($Vs_{(COO)}$); ^{1}H NMR (δ):10.15 (s,1H);7.24 (t, J = 2.0Hz,1H); 7.09 (t, J = 8.0Hz,1H); 6.95 (d, J= 8.0,2.0 Hz,1H); 6.48 (d, J = 8.0,2.0 Hz,1H); 3.46 (s, 4H); 3.54 (s, 2H); ESI-MS: *m/z* 281 $[M-1]^-$, MW calc. ($C_{12}H_{14}O_6N_2$) 282.25.

Vanadyl N-(hydroxyphenylcarbamoylmethyl) iminodiacetate (VOhpada) (**4a,b,c**). Compound **3a,b,c** (9.52 mmol) was dissolved in 25 mL deionized waters. Then freshly prepared vanadyl (IV) hydroxide (2.02 g) was added and the solution was left with stirring for 2 h at room temperature. The unreacted vanadyl (IV) hydroxide was removed by filtration.

Finally, the product was obtained by recrystallization.

4a (VOphpada): Dark blue-gray; Yield 63.99%; IR (cm^{-1}): 3342 cm^{-1} ($V_{(O-H)}$);1635 cm^{-1}, 1399 cm^{-1}, 808 cm^{-1} (ring $V_{C=C}$); 1635 cm^{-1} ($Vas_{(COO)}$); 1370 cm^{-1}($Vs_{(COO)}$); 974 cm^{-1}($V_{V=O}$); UV-VIS (H_2O,pH 5) (λ(nm) (ε (M^{-1}·cm^{-1}))): 800(94), 597(55); ESI-MS (negative ion mode): m/z 364 $[M-1]^-$; Elemental Analysis (%): C 39.58;N 7.6; Anal. Calc. VO(H_2O)L:C 39.58; N 7.69.

4b (VOmhpada): Dark blue-gray; Yield 72.61%; IR (cm^{-1}): 3434 cm^{-1} ($V_{(O-H)}$); 1617 cm^{-1}, 1480 cm^{-1} (ring $V_{C=C}$); 1632 cm^{-1} ($Vas_{(COO)}$); 1417 cm^{-1} ($Vs_{(COO)}$); 974 cm^{-1}($V_{V=O}$); UV-VIS (H_2O,pH 5) (λ(nm) (ε (M^{-1}·cm^{-1}))): 846(102), 625(56); ESI-MS (negative ion mode): *m/z* 364 $[M-1]^-$; Elemental Analysis (%): C 39.58;N 7.6; Anal. Calc. VO(H_2O)L: C 39.5;N 7.78.

4c (VOohpada): Dark blue-gray; Yield 76.76%; IR (cm^{-1}): 3434 cm^{-1} ($V_{(O-H)}$); 1600 cm^{-1}, 1480 cm^{-1},779 cm^{-1} (ring $V_{C=C}$); 1632 cm^{-1} ($Vas_{(COO)}$); 1453 cm^{-1} ($Vs_{(COO)}$); 971($V_{V=O}$); UV-VIS (H_2O,pH 5) (λ(nm) (ε (M^{-1}·cm^{-1}))): 826(107), 597(55); ESI-MS (negative ion mode): *m/z* 364 $[M-1]^-$; Elemental Analysis (%): C 39.25; N 7.93, Anal. Calc. VO(H_2O)L: C 39.5; N 7.78.

2.3. *In vitro tests of antioxidant activity*

The antioxidant activity of vanadium complexes and free ligand was tested by hydroxyl radical scavenging capacity (HRSC) as previously described [36]. Briefly, antioxidants at various concentrations were added to the Fenton reaction media containing 0.01 mM Rhodamine B, 1.0 mM $FeSO_4$, 5.0 mM of cetyl trimethyl ammonium bromide (CTAB), and 20 mM acetic acid (pH 2.8). After addition of 2.0 mM (final concentration) of H_2O_2, the

reactions were left for 10 min at room temperature. Then absorbance A_s at 550 nm was measured. The antioxidant recovery capacity R was calculated as:

$$R = (A_S - A_b)/(A_0 - A_b)$$

Where A_0 is the control ($c_{antioxidant} = 0$) and A_b is the reagent blank. Then the data was further fitted to the following equation:

$$\frac{1}{R} = \frac{1}{c_{antixidant}} \frac{K}{k \cdot R_{max}} + \frac{1}{R_{max}}$$

Then R_{max} and k/K were obtained using an Origin™ 7.2 program. HRSC index was calculated by setting the k/K value of ascorbic acid as 1.0.

2.4. *Cytotoxicity on HK-2 human kidney cells*

The cytotoxicity of vanadium complexes on HK-2 cells were conducted using the MTT (3-(4,5-Dimethylthiazol-2-yl)-2,5-diphenyltetrazolium bromide) assay [37]. Briefly,4~5×10^3 cells were plated onto 96-well plates (Corning, USA). Upon confluence, the cells were incubation with different concentrations of vanadium complexes for 24 h at 37 °C. Then, MTT reagent was added to the cells according to the manufacturer protocol and the absorbance at 570 nm was measured with a microplate reader (Multiskan Mk3; Thermo Labsystems, Vantaa, Finland).

2.5. *Animal treatments*

Male C57BLKS/J diabetic obese (*db/db*) mice (8 weeks) were from Model Animal Research Center of Nanjing University and housed under controlled temperature (23 °C) and lighting (12 h lighting between 6 A.M. and 6 P.M.) with free access to water and standard mouse diet. All care and handling of animals were performed with the approval of

Institutional Review Board for Laboratory Animal Care (Approval No. LA2010-052).

When the fasting blood glucose levels of mice reached ≥12 mM, a total of 28 mice randomly divided into four groups: Group I, Control diabetic mice (*n*=7); Group II, BMOV-treated diabetic mice (*n*=7, 0.1 mmol/kg/day); Group III, Compound **4a** (VOphpada) treated diabetic mice (*n*=7, 0.1 mmol/kg/day); Group IV, Ligand (Compound **3a**, *p*-H_2hpada)-treated mice (*n*=7, 0.1 mmol/kg/day). The BMOV-treated group was considered as the positive control group.

To avoid any irritation by oral gavage, vanadium treatments for *db*/*db* mice were conducted by feeding the animal with pellet food containing desired amounts of vanadyl complexes as described previously [38]. Throughout the experimental period, the body weight, food and water intake were monitored. Blood samples were obtained from the tail vein of the mice and blood glucose levels were determined with an Accu-Chek blood glucose monitor (Roche Diagnostics GmbH, Mannheim, Germany). At the end of the study, the animals were euthanized and tissue samples of muscle, fat, livers and kidney were taken off for further analysis.

2.6. *Glucose tolerance tests (OGTT)*

At the end of experiment, OGTT was performed. Briefly, the mice were fasted for 12 h, and glucose (200 $mg*mL^{-1}$) was delivered by oral gavage at a dose of 2 $g*kg^{-1}$. Blood samples were available from the tail vein at 0, 5, 15, 30, 60, 120 and 180 min after glucose loading. The blood glucose levels were monitored with an Accu-Chek blood glucose monitor (Roche Diagnostics GmbH, Mannheim, Germany).

2.7. *Serum biochemical parameters test*

The mice were fasted for 12 h and serum was prepared from the orbit blood sampling for determination of biochemical parameters in serum including total cholesterol (TCHO), triglycerides (TG), alanine aminotransferase (ALT), aspartate transaminase (AST), creatinine (Cre), blood urea nitrogen (BUN), and albumin (Alb). Since the volume of blood sample from single mouse was not enough for sample loading, an equivalent volume mixture of all seven samples in the same treated group were applied to an OLYMPUS AU400 clinical chemistry analyzer (Olympus, Tokyo, Japan) with the assay kits from Randox (Antrim, UK).

2.8. *PCR assay for PPARs expression*

Total RNA was separated from mice muscle and fat with a TRIzol extraction kit (Invitrogen). After quantification of extracted RNA pellets with an BioPhotometer 6131 (Eppendorf, Germany), first-strand complementary DNA synthesis was performed using a Superscript First Strand Synthesis Kit (Invitrogen). All samples were analyzed with a quantitative real-time PCR (Eppendorf, Germany) using SYBR Green contained PCR Master Mix (Applied Biosystem, Inc.USA) according to the manufacturer protocol. The mRNA expression levels of all genes were normalized to that of GAPDH in the same sample, and then the relative differences between the diabetic control group and the treatment groups were calculated and expressed as relative increases, with the control value set to 100%.

The primer sequences are listed as follow:

	Primer sequences
PPARα	Forward primer 5'-TCACACAATGCAATCCGTTT-3'

	Reverse primer 5'-GGCCTTGACCTTGTTCATGT-3'
PPARγ	Forward primer 5' -GTGAAGTTCAACGCACTGGA-3’
	Reverse primer 5'-ATGTCCTCAATGGGCTTCAC-3'
GAPDH	Forward primer 5'-GACTTCAACAGCAACTCCCAC-3'
	Reverse primer 5'-TCCACCACCCTGTTGCTGTA-3’

2.9. *Western blotting analysis*

The frozen tissues were homogenized in a lysis buffer (20 mM Tris-HCl, 150 mM NaCl, 1 mM EDTA, 1 mM EGTA, 1% TritonX-100 and protease inhibitor, pH 7.4) and then centrifuged (12,000 rpm) at 4°C for 25 min to discard tissues debris. The supernatants were collected and protein concentrations were measured using a BCA Protein Assay kit (Pierce, Rockford, IL, US). Samples containing 40 μg total proteins were applied to a 10% SDS-PAGE and then subjected to desire antibodies after transfer to a polyvinylidene difluoride (PVDF) membrane (Millipore Corp, Atlanta, GA, US). The membrane was blocked for 1 h with Tris-buffered saline containing 0.1% Tween 20 and 5% bovine serum albumin and then incubated with desired primary antibodies overnight at 4°C followed by a horseradish peroxidase (HRP)-conjugated secondary antibodies (1:10,000) at room temperature for 1 h. The protein bands were developed with a ChemiDoc XRS kit (Bio-Rad, USA) on an X-ray film (Kodak, Fujian, China) according to the specification of manufacturer. Protein expression results were analyzed and quantified using a Scion Image Software (Scion, Frederick, MD).

2.10. *Acute oral toxicity of VOphpada in mice*

The acute oral toxicity study was conducted according to the method of Ref. [39]. Briefly, healthy ICR mice were divided randomly into six groups (n=10). After 12 h fasting, each group of mice were given were administered as suspensions in double distilled water (ddH_2O) intragastrically at doses of 1735, 1400, 1120, 896, 716.8, 573 $mg*kg^{-1}$ body weight according to the dosage ratio of 1:0.8 among groups, with ddH_2O as control. After vanadium administration, the mice were fed normally and observed successively for mortality for 14 days and the LD_{50} value were calculated.

2.11. *Statistical analysis*

All data are presented as means±SD. Each experiment was performed at least in triplicate. The statistical analysis was performed by one-way analysis of variance (ANOVA) followed by Dunnett's multiple comparison tests using a SPSS™ 13.0 software and an Origin™ 7.2 program. Statistical significance was accepted at the level of p<0.05.

3. Results

3.1. *Synthesis*

The vanadium complexes (**4a~c**) were prepared from ligands (**3a~c**) as described above. The three complexes are well water soluble. The IR data revealed a peak at ~974 cm^{-1}, which is in the region (930-1030 cm^{-1}) of characteristic V^{IV}=O stretching frequencies [31, 40, 41], confirm the formation of vanadyl complexes. The UV-VIS spectra (Fig.1) of three V^{IV}O-hpada complexes are similar to those of $[VO(H_2O)nta]^-$ [42-44] and its analogs[45] and are consistent with the tetragonally compressed symmetry commonly associated with spectra of the vanadyl ion and its complexes [45]. The results of elemental analysis agreed with a

formula of $V^{IV}O(H_2O)L$ for the complexes. In ESI mass spectra, three related peaks were observed at *m/z* 346, 363, 364. The peaks at *m/z* 346 and 363 correspond to the formula of $V^{IV}OL$ and $V^{V}O(OH)L$, respectively. While the peak at *m/z* 364, shown as a shoulder of peak *m/z* 364, is the $[M-1]^-$ molecular ion peak for $V^{IV}O(H_2O)L$. It is possible that in the process of sampling and/or mass analysis, most complexes may either loose a water molecule or be oxidized to +5 valence complexes. According to the crystal and solution structures of a series of mononuclear vanadium (IV) complexes with nitrilotriacetate and iminodiacetate derivatives [45] , the formula of vanadyl complexes were assigned to be $V^{IV}O(H_2O)L$.

[Fig.1]

3.2. *Determination of pK_{a1}(OH) value*

The equilibrium constant for dissociation of coordination water (1) is a very important molecular property for susceptibility and rate of oxidation to V^V [42, 46]:

$$VO(H_2O)L \underset{\longleftarrow}{\xrightarrow{pKa1(OH)}} VO(OH)L^- + H^+ \quad (1)$$

Thus, the pK_{a1}(OH) values of the three $V^{IV}O$-hpada complexes **4a~c** were determined by pH-dependent spectrophotometric measurements as described in Materials and Methods. The pH-dependent spectra and titration curve for $V^{IV}O$-hpada complexes are shown in Fig. 2. The pK_{a1}(OH) values were calculated to be 7.4±0.2, 6.5±0.1 and 7.6±0.4. for VOphpada , VOmhpada and VOohpada , respectively. These values for $V^{IV}O$-hpada complexes are close to that of $[V^{IV}O(H_2O)nta]^-$ (pK_{a1}(OH) =6.9) [46].

[Fig. 2.]

3.3. *In vitro antioxidant activity*

The antioxidant activity of vanadium complexes **4a~c** and the ligands was estimated as hydroxyl radical scavenging capacity (HRSC) (Table 1). Compound **4a** (VOphpada) gave the best HRSC index among the complexes and ligands. In addition, VOphpada exhibited significantly better antioxidant activity than its ligand.

[Table 1]

3.4. *Cytotoxicity on kidney cells*

The in *vitro* cytotoxicity of vanadyl complexes **4a~c** on HK-2 cells was tested and the IC_{50} were calculated in Table 2. The complex **4a** (VOphpada) showed significantly lower toxicity than the other analogs, its parental compound (VOimda) and the reference compound BMOV.

[Table 2]

3.5. *Median lethal dose of VOphpada*

The results of acute oral toxicity were listed in Table 3. The oral LD_{50} of VOphpada was calculated to be 1045 $mg{*}kg^{-1}$. According to Loomis and Hayes classification [47] , chemical substance with a LD_{50} within the range of 5,000–15,000 $mg{*}kg^{-1}$, 500–5,000 $mg{*}kg^{-1}$, 50–500 $mg{*}kg^{-1}$, and 1–50 $mg{*}kg^{-1}$ is regarded as practically nontoxic, slightly toxic, moderately toxic, and highly toxic, respectively. Compound **4a** (VOphpada) is in the category of slightly toxic substance.

[Table 3]

3.6. *The effects of compound **4a** (VOphpada) on animal growth of db/db mice*

The daily food and water intake of animals were shown in Fig. 3. At the treatment dose,

both BMOV and VOphpada did not decrease animal'appetite while BMOV and phpada ligand slightly increased food intake. While the daily water intake for vanadium treated mice was significantly lower than that of diabetic control, indicating the improvement of glucose metabolism of the animals. In agreement with the food and water consumption, the body weight of the treated groups steadily increased (Fig.4) and the treated mice were significantly heavier than the diabetic control.

[Fig. 3]

[Fig.4]

3.7. *Blood glucose level and Glucose tolerance test*

Compared with the diabetic control, the blood glucose of *db/db* mice treated with vanadium complexes (0.1 mmol/kg/day) decreased gradually to normal range (<12 mM) (Fig.5). The glucose tolerance was also improved with significance (Fig.6) after 6-weeks vanadium treatment. Obviously, compound **4a** (VOphpada) produced much stable hypoglycemic effect than BMOV in *db/db* mice. Interestingly, the ligand **3a** (H_2hpada) alone did not decrease glucose level, however, somewhat improved glucose tolerance of the diabetic animals (Fig.6).

[Fig.5]

[Fig.6]

3.8. *Serum biochemical parameters*

As shown in Table 4, treatment with vanadium complexes greatly reduced the levels of AST, ALP, BUN, and Cre, indicating that vanadium treatment alleviated the injuries in liver,

heart, and kidney caused by hyperglycemia. The effects of compound **4a** (VOphpada) is essentially similar to those of BMOV.

[Table 4]

3.9. *Effects of vanadium compounds on PPARs transcription in muscle and fat*

As shown in Fig.7, treatment with vanadium compounds increased mRNA levels of PPARα in muscle and both PPARα and PPARγ in fat. The compound **4a** (VOphpada) exhibited much stronger enhancement than BMOV. While the ligand **3a** alone caused decrease of mRNA levels of PPARα and/or PPARγ.

[Fig.7]

3.10. *Effects of vanadium treatment on AKT, PPARα, PPARγ, and pJNK, in muscle and fat tissues*

As shown in Fig.8, vanadium treatment caused elevation of Akt/PKB, PPARα and PPARγ while decrease phosphorylation activation of JNK (pJNK) in both muscle and fat tissues. Interestingly, vanadium complexes activated more PPARα in muscle but more PPARγ in fat. In overall, the effects of compound **4a** were significantly stronger than BMOV. In contrast, the ligand **3a** alone did not significantly affect Akt/PKB, PPARα or PPARγ.

[Fig.8]

3.11. *The effect of vanadium complexes on kidney injury molecule-1 (TIM-1/KIM-1)*

The renal toxicity of vanadium complexes was investigated by measuring the level of TIM-1/KIM-1 marker. As shown in Fig.9, neither vanadium complexes nor the ligand **3a**

caused increase of TIM-1/KIM-1 expression. However, VOphpada slightly reduced TIM-1/KIM-1 level with significance.

[Fig.9]

4. Discussion

The vanadyl complexes with derivatives of nitrilotriacetic acid or iminodiacetic acid have been thoroughly investigated as models of inactive form of vanadium haloperoxidases. Considering the structural homology of vanadyl nitrilotriacetate to vanadyl dipicolinate complexes, we proposed that vanadyl complexes with nitrilotriacetic acid derivatives could exhibit good hypoglycemic effect. In addition, vanadyl nitrilotriacetate exhibits high water solubility and small molecular size. Therefore, we designed and synthesized the novel aminophenol-derivatized nitrilotriacetic acid vanadyl complexes. Spectroscopic characterization gave the formula of $V^{IV}O(H_2O)L$ as expected. Nevertheless, fully characterization of the solution chemistry of the complexes (e.g. pH-metric chemical speciation, redox potential and plasma protein binding, etc.) would be appropriate for further works. It has been suggested that the solution stability, the ability to interact with cellular redox reactions, and the capacity to remain intact upon binding to serum albumin may be crucial for the insulin-enhancing activity of Vdipic complexes [48] .

The toxicity of the complexes was firstly evaluated in *vitro* on HK-2 kidney cells (Table 2) along with their antioxidant capacity (Table 1). It is noted that: (***i***) the cytotoxicity of VOphpada (**4a**) is lower than BMOV; (***ii***) similar to the acute toxicity of BSOV analogs [31],

the toxicity of three aminophenol-derivatized nitrilotriacetic acid vanadyl complexes (**4b**>**4c**>**4a**) again show an inversed relationship with their antioxidant activities (**4b**<**4c**<**4a**); (***iii***) the *p*-aminophenol derivative VOphpada showed an increased antioxidant activity over its ligand *p*-H_2phpada while its cytotoxicity was significantly lower than the parental complex (VOimda). In contrast, complexes **4b** and **4c** showed decreased antioxidant activities over their ligands and their cytotoxicity was significantly higher than the reference. This suggests that the position of the hydroxyl group could exert significant impact on the redox behaviors of the complexes. It is also possible that vanadyl complexes with antioxidant activity higher than their ligands normally give lower cytotoxicity and vice versa. Nevertheless, the exact structural effects and underlying mechanisms need to be investigated in further works.

Based on the above evaluations of complex susceptibility, antioxidant activity and renal cytotoxicity, VOphpada was chosen to test its anti-diabetic therapeutic potential and animal toxicity. Herein, the vanadium complexes was administrated in pellet food to avoid any gastrointestinal irritation under a dose (0.1 mmol/kg/day) without any feeding suppression. Therefore, mice in treated groups consumed equal amount of more food than the diabetic control (Fig.3). Both BMOV and VOphpada significantly reduced blood glucose level (Fig.5) and thus water consumption (Fig.3B). However, VOphpada was obviously more effective than BMOV in improving glucose tolerance (Fig.6). Interestingly, the ligand (*p*-H_2hpada) alone also showed a weak capacity of ameliorating blood glucose status (Fig.5&6), possibly due to antioxidant activity like that of resveratrol [49] . Consequently, the animals in all three treated groups generated more body growth than the diabetic control.

The levels of serum biomarkers in Table 4 revealed the changes of health status during the treatment. Although *db*/*db* mice exhibited hyperglycemia and hyperlipidemia (Chol and TG), the mice maintained fairly normal liver (ALT, AST, and ALP) and kidney (Cre) functions compared with the healthy C57BL/6 mice. However, the elevated BUN level and reduced serum albumin (Alb) indicated significant high level of protein degradation, a typical sign of stress caused by hyperglycemia and/or hyperlipidemia. Treatment with BMOV or VOphpada ameliorated blood glucose (Fig.5&6) and lipid levels, and reduced BUN level (especially the BUN/Cre ratio) to normal ranges indicating the effective relief of hyperglycemic stress upon vanadium treatment. But vanadium treatment did not improve much on Alb level. Previously, we observed that vanadyl complexes reduced insulin synthesis on β-cells upon high glucose stimulation through induction of unfolded protein responses [39]. It is possible that vanadium treatment may restrict general protein synthesis via a similar mechanism. Considering the role of albumin in maintaining the serum colloid osmotic pressure, long term low serum albumin could alter renal function. However, it was also observed that Alb levels in groups with increased food consumption (BMOV and *p*-H_2hpada groups) were notably improved, suggesting that dietary modification (e.g. addition of leucine or its metabolite β-hydroxy-β-methylbutyrate) to promote protein synthesis may be a potential solution of this side effects of vanadium treatment for the future studies.

PCR and western blot analysis (Fig.7&8) revealed that both BMOV and VOphpada exhibited hypoglycemic effect through insulin enhancing mechanism: (***i***) both vanadyl complexes caused significant elevation of Akt, indicating activation of insulin signal

transduction; (***ii***) both treatment increased expression of PPARα and γ, primarily in muscle and adipose tissue, respectively. Different from in *vitro* s tudies [50, 51] that vanadium compounds elevated PPARγ expression exclusively by suppressing protein degradation, vanadyl complexes here in animals acted at both transcriptional and post-translational levels. PPARα and γ are well recognized targets for insulin enhancers [52], e.g. rosiglitazone. Increase of PPARα and γ activity can significantly improve lipid and glucose metabolism [52] ; (***iii***) as the consequence of PPARγ activation [52] , vanadium treatment significantly reduced phosphorylation of JNK (c-Jun NH_2-terminal protein Kinase). JNK belongs to the stress-activated protein kinase family [38, 53]. Phosphorylation of IRS1 (insulin receptor substrate-1) by JNK will cause down-regulation of insulin signaling; this has been regarded as one major mechanism for insulin resistance [53]. Thus, inactivation of JNK by vanadium treatment should play an important role in the insulin enhancement action of vanadyl complexes. Again, VOphpada exhibited more potent effects than BMOV.

Toxicity, especially renal side effect, is currently the most concern for anti-diabetic vanadyl complexes. As in Table 3, VOphpada is a slightly toxic substance, exhibiting a similar cute oral toxicity (LD_{50} = 1045 $mg*kg^{-1}$) to that of BMOV (LD_{50} = 902 $mg*kg^{-1}$) [31]. The six-week treatment with BMOV and VOphpada (Fig.9) did not cause significant elevation of the kidney injury molecule-1 (TIM-1/KIM-1); while VOphpada even slightly reduced TIM-1/KIM-1 level, suggesting potentially lower long term toxicity of VOphpada. However, considering the potential of vanadium-induced inflammatory responses (not investigated herein) and possible consequences of low serum albumin (if last ever), the long

term renal toxicity of VOphpada needs to be carefully investigated in future works.

5. Conclusion

In the present work, we reported design and synthesis of novel aminophenol-derivatized nitrilotriacetic acid vanadyl complexes. The position of the hydroxyl group was observed significantly influence the antioxidant activity and cytotoxicity of the vanadyl complexes; while VOphpada exhibited a high antioxidant activity and fairly low cytotoxicity. In a type II diabetic model, VOphpada exhibited significantly more potent insulin enhancement effects than BMOV while showing similar short term toxicity. Further works on long term renal toxicity would be appropriate for the development of VOphpada as novel hypoglycemic agent. Nonetheless, the present results suggest that proper incorporation of antioxidant groups in ligand could lead to vanadyl complexes with improved balance between the therapeutic properties and the side effects.

Abbreviations

BMOV	bis(maltolato)oxovanadium
BEOV	bis(ethylmaltolato)oxovanadium (IV)
BSOV	bis((5-hydroxy-4-oxo-4H-pyran-2-yl)methyl2-hydroxybenzoatato)oxovanadium(IV)
H_2hpada	N-(hydroxyphenylcarbamoylmethyl) iminodiacetic acid
VOhpada	Vanadyl N-(hydroxyphenylcarbamoylmethyl) iminodiacetate

TG	triglycerides
ALT	alanine aminotransferase
AST	aspartate transaminase
Cre	creatinine
BUN	blood urea nitrogen
Alb	albumin
TCHO	total cholesterol
OGTT	glucose tolerance test.
PPAR-γ	peroxisome proliferator-activated receptor-γ
PPAR-a	peroxisome proliferator-activated receptor-a
AKT(PKB)	Protein kinase B
pJNK	PhosphoJun N-terminal kinase
GAPDH	glyceraldehyde-3-phosphate dehydrogenase

Acknowledgements

Project (No. 21271012) supported by NNSFC.

References

[1] K.H. Thompson, J. Lichter, C. LeBel, M.C. Scaife, J.H. McNeill, C. Orvig, J. Inorg. Biochem.103 (2009) 554-558.

[2] M. Huang, Y. Wu, P. Zhao, X. Yang, Prog Chem.25 (2013) 650-660.

[3] K.H. Thompson, C. Orvig, J. Inorg. Biochem.100 (2006) 1925-1935.

[4] H.Sakurai, K.Fujii, H.Watanabe, H.Tamura, Biochem. Biophys. Res. Commun.214 (1995) 1095-1101.

[5] K. Fukui, Y. Fujisawa, H. OhyaNishiguchi, H. Kamada, H. Sakurai, J. Inorg. Biochem.77 (1999) 215-224.

[6] H. Esbak, E.A. Enyedy, T. Kiss, Y. Yoshikawa, H. Sakurai, E. Garribba, D. Rehder, J. Inorg. Biochem.103 (2009) 590-600.

[7] H. Sakurai, A. Katoh, T. Kiss, T. Jakusch, M. Hattori, Metallomics.2 (2010) 670-682.

[8] P. Buglyo, D.C. Crans, E.M. Nagy, R.L. Lindo, L. Yang, J.J. Smee, W. Jin, L.H. Chi, M.E. Godzala Iii, G.R. Willsky, Inorg Chem.44 (2005) 5416-5427.

[9] J.J. Smee, J.A. Epps, K. Ooms, S.E. Bolte, T. Polenova, B. Baruah, L. Yang, W. Ding, M. Li, G.R. Willsky, A. la Cour, O.P. Anderson, D.C. Crans, J. Inorg. Biochem.103 (2009) 575-584.

[10] M. Xie, D. Chen, F. Zhang, G.R. Willsky, D.C. Crans, W. Ding, J. Inorg. Biochem.136 (2014) 47-56.

[11] C. John., http://www.fiercebiotech.com/story/akesis-shutters-program-files-chap-7/, 2009-01-22.

[12] K. Gruzewska, A. Michno, T. Pawelczyk, H. Bielarczyk, J. Physiol. Pharmacol.65 (2014) 603-611.

[13] Y. Zhao, L. Ye, H. Liu, Q. Xia, Y. Zhang, X. Yang, K. Wang, J. Inorg. Biochem.104 (2010) 371-378.

[14] M. Aureliano, Dalton Trans.42 (2009) 9093-9100.

[15] J. Korbecki, I. Baranowska-Bosiacka, I. Gutowska, K. Piotrowska, D. Chlubek, Biol. Trace

Elem. Res.163 (2015) 103-111.

[16] H. Tang, Y. Sun, Q. Xiu, H. Lu, H. Han, Arch. Biochem. Biophys.468 (2007) 92-99.

[17] D. Ha, H. Joo, G. Ahn, M.J. Kim, S.J. Bing, S. An, H. Kim, K.G. Kang, Y.K. Lim, Y. Jee, Food. Chem. Toxicol.50 (2012) 2097-2105.

[18] Z. Xu, X. Wang, R. Xiao, X. Yang, J. Pharm. Pharmacol.22 (2013) 403-408.

[19] K. Azami, K. Tabrizian, R. Hosseini, M. Seyedabadi, M. Shariatpanahi, F. Noorbakhsh, A. Kebriaeezadeh, S.N. Ostad, M. Sharifzadeh, Neurotoxicology.33 (2012) 44-52.

[20] G. Fraqueza, L.A.B. Carvalho, M.P. Marques, L. Maia, C.A. Ohlin, W.H. Casey, M. Aureliano, DALTON.T.41 (2012) 12749-12758.

[21] R. Shukla, V. Barve, S. Padhye, R. Bhonde, Bioorg. Med. Chem. Lett.14 (2004) 4961-4965.

[22] R. Shukla, S. Padhye, M. Modak, S.S. Ghaskadbi, R.R. Bhonde, Rev. Diabet. Stud.4 (2007) 33-43.

[23] R. Shukla, V. Barve, S. Padhye, R. Bhonde, Biometals.19 (2006) 685-693.

[24] S.I. Pillai, S.P. Subramanian, M. Kandaswamy, Eur. J. Med. Chem.63 (2013) 109-117.

[25] S.I. Pillai, S.P. Subramanian, M. Kandaswamy, Chem. Biol. Interact.204 (2013) 67-74.

[26] L. Naso, E.G. Ferrer, L. Lezama, T. Rojo, S.B. Etcheverry, P. Williams, J. Biol. Inorg. Chem.15 (2010) 889-902.

[27] D. Sanna, V. Ugone, G. Lubinu, G. Micera, E. Garribba, J. Inorg. Biochem.140 (2014) 173-184.

[28] I.E. Leon, V. Porro, A.L. Di Virgilio, L.G. Naso, P.A. Williams, M. Bollati-Fogolin, S.B. Etcheverry, J. Biol. Inorg. Chem.19 (2014) 59-74.

[29] I.E. Leon, A.L. Di Virgilio, V. Porro, C.I. Muglia, L.G. Naso, P.A. Williams, M. Bollati-Fogolin, S.B. Etcheverry, DALTON.T.42 (2013) 11868-11880.

[30] D. Vernardou, D. Louloudakis, E. Spanakis, N. Katsarakis, E. Koudoumas, New J. Chem.38 (2014) 1959-1964.

[31] Y. Wei, C. Zhang, P. Zhao, X. Yang, K. Wang, J. Inorg. Biochem.105 (2011) 1081-1085.

[32] Y.B. Wei, X.D. Yang, Biometals.25 (2012) 1261-1268.

[33] P. Caravan, L. Gelmini, N. Glover, F.G. Herring, H. Li, J.H. McNeill, S.J. Rettig, I.A. Setyawati, E. Shuter, Y. Sun, A.S. Tracey, V.G. Yuen, C. Orvig, J. Am. Chem. SOC. 117 (1995) 12759-12770.

[34] D.C. Crans, J.J. Smee, E. Gaidamauskas, L. Yang, Chem. Rev.104 (2004) 849-902.

[35] X.R. Zhao, C.X. Li, ASNUP.38 (2002) 175-180.

[36] F.Yu, D.Xu, R.Lei, N.Li, K.Li, J. Agric. Food Chem.56 (2008) 730–735.

[37] F. Denizot, R. Lang, J. Immunol. methods.89 (1986) 271-277.

[38] M. Huang, Y. Wu, N. Wang, Z. Wang, P. Zhao, X. Yang, Biol. Trace Elem. Res.157 (2014) 242-248.

[39] Z. Gao, C. Zhang, S. Yu, X. Yang, K. Wang, J. Biol. Inorg. Chem.16 (2011) 789-798.

[40] S. Kundu, S. Maity, A.N. Maity, S.C. Ke, P. Ghosh, DALTON.T.42 (2013) 4586-4601.

[41] A.R. Sarkar, S. Mandal, Met.-Based Drugs.7 (2000) 157-164.

[42] M. Nishizava, Y. Sasaki, K. Saito, B. Bruni, Inorg. Chem.24 (1985) 767-772. .

[43] M. Nishizawa, K. Hirotsu, S. Ooi, K.J. Saito, J.C.S. CHEM. COMM. (1979) 707-708.

[44] R. Meier, G. Werner, M. Otto, Collect. Czech. Chem. Commun. 54 (1989) 64-69.

[45] B.J. Hamstra, A.L.P. Houseman, G.J. Colpas, J.W. Kampf, R. LoBrutto, W.D. Frasch, V.L. Pecoraro, Inorg. Chem.36 (1997) 4866-4874.

[46] R. Meier, G. Werner, M. Otto, Collect. Czech. Chem. Commun.54 (1989) 64-69.

[47] T.A. Loomis, A.W. Hayes (Eds.), Loomis's essentials of toxicology, Academic Press, 1996.

[48] M.W. Makinen, M. Salehitazangi, Coord. Chem. Rev.279 (2014) 1-22.

[49] J.K. Bhatt, S. Thomas, M.J. Nanjan, AM.J.Physiol-Reg.I.32 (2012) 537-541.

[50] P. Zhao, X.D. Yang, Metallomics.5 (2013) 836-843.

[51] Y. Wu, M. Huang, P. Zhao, X. Yang, J. Biol. Inorg. Chem.18 (2013) 623-631.

[52] M. Ricote, C.K. Glass, Biochim. Biophys. Acta.1771 (2007) 926-935.

[53] J. Hirosumi, G. Tuncman, L. Chang, C.Z. Gorgun, K.T. Uysal, K. Maeda, M. Karin, G.S. Hotamisligil, Nature.420 (2002) 333-336.

[54] D.P. Wang, S.R. Li, M. Zhang, S.T. Li, Y.P. Zhang, Z.X. Geng, R.F. Li, Lab. Anim. Sci. Admin.17 (2000) 25-28.

Table 1. Hydroxyl radical scavenging capacity (HRSC) of vanadium complexes and the ligands.

Compounds	R_{max}	k/K	r^2	HRSC index
L-ascorbic acid	2.30	0.404	0.9904	1
ligand **3a**	0.466	30.7	0.9753	76.0
Complex **4a** (VOphpada)	0.912	36.8	0.9037	91.2
ligand **3b**	0.678	15.8	0.9475	39.1
Complex **4b**	1.75	2.45	0.9357	6.08
ligand **3c**	0.670	13.9	0.9700	34.5
Complex **4c**	1.60	2.71	0.9399	6.71

Table 2. Half inhibition concentration (IC_{50}) of vanadium complexes **4a~c** on HK2 cells.

Compounds	IC_{50} (μM)
4a (VOphpada)	470 ± 47
4b	20 ± 2
4c	71 ± 15
BMOV	333 ± 29
Vanadyl iminodiacetate (VOimda)	136 ± 27

Table 3. Acute toxicity results of **4a** (VOphpada) in mice

Groups	Mice number	Dosage ($mg*kg^{-1}$)	Log(dosage)	Number of death	Rate of death (%)
1	10	1,735	3.24	10	100
2	10	1,400	3.15	9	90
3	10	1,120	3.05	7	70
4	10	896	2.95	5	50
5	10	717	2.86	2	20
6	10	573	2.76	0	0

Table 4. Effects of VOphpada on serum biochemical parameters in *db/db* diabetic mice[1].

	Diabetic control	BMOV	*p*-H_2hpada	VOphpada	Normal range (C57BL/6 mice)[2]
ALT ($U*L^{-1}$)	60	77	83	63	40-70
AST ($U*L^{-1}$)	168	134	221	80	80-170
ALP ($U*L^{-1}$)	114	105	122	102	110-160
BUN (mM)	35.1	7.7	7.9	8.9	5-13
Cre ($mg*dL^{-1}$)	74	40	38	44	20-110
Chol (mM)	4.33	3.56	2.63	3.46	0.7-2.1
TG (mM)	2.12	1.13	1.34	1.90	0.5-1.7
Alb ($g*L^{-1}$)	21.4	24.3	24.8	21.7	28-32

[1]Due to the need for large sample size, an equivalent volume mixture of all seven samples in a group were applied to an OLYMPUS AU400 clinical chemistry analyzer

[2]Data from Ref. [54].

Fig.1 The UV-VIS spectra of three $V^{IV}O$-hpada complexes at pH≈5 aqueous solution (complex concentration:5 mM). VOphpada, Dash dot dot line (λ_{max}: 800 and 597 nm); VOmhpada,Solid line (λ_{max}: 846 and 625 nm); VOohpada,Dash line(λ_{max}: 826 and 597 nm).

Fig.2 pH spectrophotometric titration of $V^{IV}O$-hpada complexes. (A), (C) and (E): pH dependent spectra of $V^{IV}O$-phpada complexes (9.0 mM), $V^{IV}O$-ohpada complexes (5.0 mM) and $V^{IV}O$-mhpada complexes (5.0 mM), respectively; (B), (D) and (F): the pH titration curve of $V^{IV}O$-phpada complexes , $V^{IV}O$-ohpada complexes and $V^{IV}O$-mhpada complexes respectively; Vanadyl complex were dissolved in 0.1 M Tris-HAc buffer and the spectra at 500-850 nm were recorded after adjusting to the indicated pH values. The pH-dependent changes of ΔA were plotted and the pK_{a1}(OH) values were calculated by data regression using an Origin™ 7.2 program.

Fig.3 The effect of VOphpada on food (A) and water (B) intake of diabetic mice. *n*=7 for each group. $^{**}p < 0.01$, $^{*}p < 0.05$. vs. diabetic control.

Fig.4 Changes of body weight during treatment with VOphpada. Control diabetic mice (—■—), BMOV-treated diabetic mice (—●—), VOphpada-treated diabetic mice (—▲—), *p*-H_2hpada-treated diabetic mice (—▼—). *n*=7 for each group.

Fig.5 Changes in blood glucose levels upon vanadium treatment. Control diabetic mice(—■—), BMOV-treated diabetic mice (—●—), VOphpada-treated diabetic mice(—▲—) ,

p-H_2hpada-treated diabetic mice(—▼—). *n*=7 for each group.

Fig.6 Oral glucose tolerance test curves. Control diabetic mice (—■—), BMOV-treated diabetic mice (—●—), VOphpada-treated diabetic mice (—▲—), ligand-treated diabetic mice(—▼—). *n*=7 for each group.

Fig.7 Effects of VOphpada on mRNA levels of PPARα and PPARγ in muscle (A) and fat tissues (B). *n*=7 for each group. $^{**}p < 0.01$, $^{*}p < 0.05$. vs. diabetic control.

Fig.8 Effects of VOphpada on Akt/PKB, PPARα, PPARγ, and pJNK in muscle (A) and fat (B). The proteins were extracted and analyzed by western blot as described in the experimental section. $^{**}p < 0.01$, $^{*}p < 0.05$. vs. diabetic control.

Fig.9 Effects of VOphpada on kidney injury molecule-1 (TIM-1/ KIM-1). The proteins were extracted and analyzed by western blot as described in the experimental section. $^{**}p < 0.01$, $^{*}p < 0.05$. vs. diabetic control.

Scheme.1 The synthesis route for vanadyl N-(hydroxyphenylcarbamoylmethyl) iminodiacetate (VOhpada).

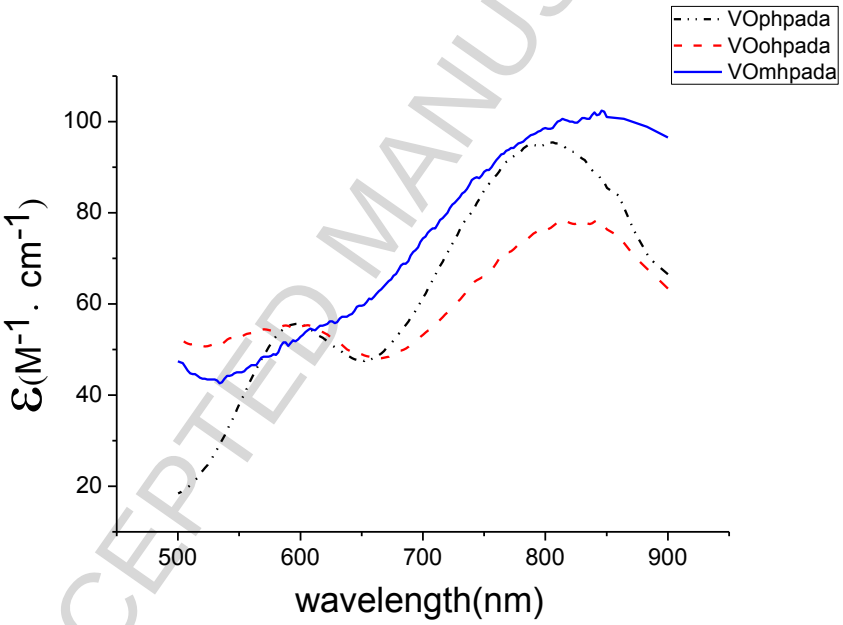

Fig.1 The UV-VIS spectra of three $V^{IV}O$-hpada complexes at pH≈5 aqueous solution (complex concentration:5 mM). VOphpada, Dash dot dot line (λ_{max}: 800 and 597 nm); VOmhpada,Solid line (λ_{max}: 846 and 625 nm); VOohpada,Dash line(λ_{max}: 826 and 597 nm).

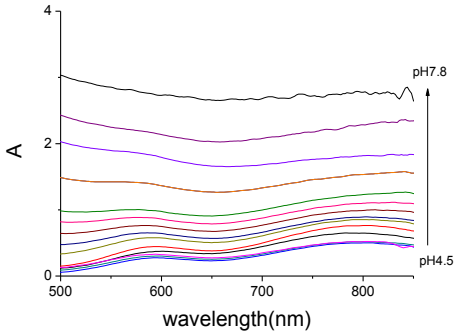

(A)

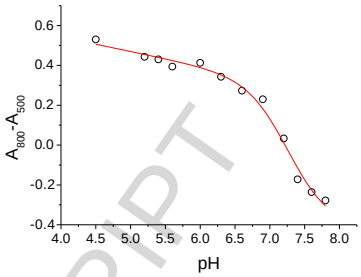

(B)

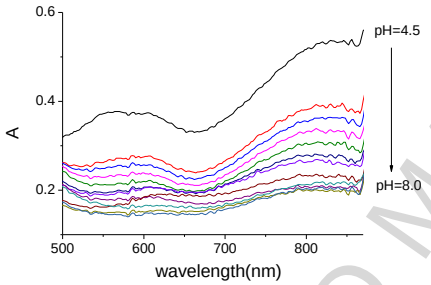

(C)

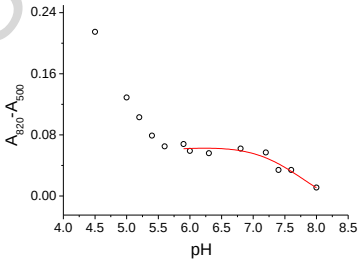

(D)

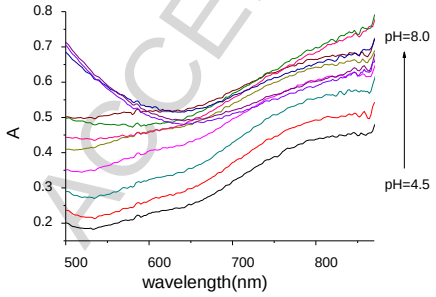

(E)

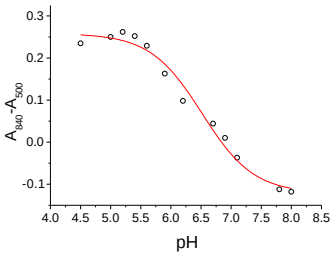

(F)

Fig.2 pH spectrophotometric titration of $V^{IV}O$-hpada complexes. (A), (C) and (E): pH dependent spectra of $V^{IV}O$-phpada complexes (9.0 mM), $V^{IV}O$-ohpada complexes (5.0 mM) and $V^{IV}O$-mhpada complexes (5.0 mM), respectively; (B), (D) and (F): the pH titration curve of

$V^{IV}O$-phpada complexes , $V^{IV}O$-ohpada complexes and $V^{IV}O$-mhpada complexes respectively; Vanadyl complex were dissolved in 0.1 M Tris-HAc buffer and the spectra at 500-850 nm were recorded after adjusting to the indicated pH values. The pH-dependent changes of ΔA were plotted and the pK_{a1}(OH) values were calculated by data regression using an Origin™ 7.2 program.

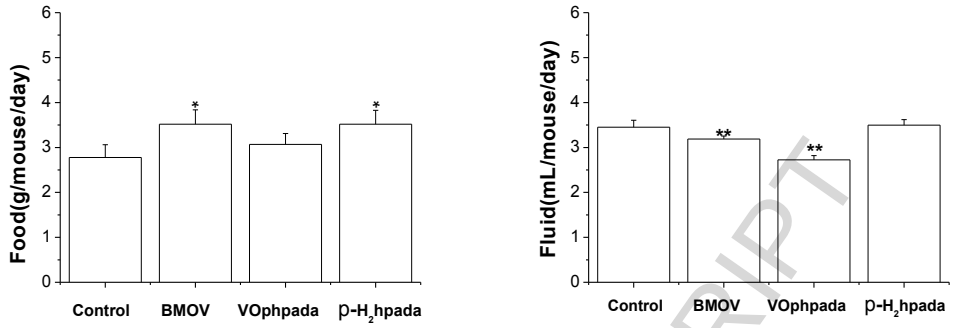

(A) (B)

Fig.3 The effect of VOphpada on food (A) and water (B) intake of diabetic mice. *n*=7 for each group. $^{**}p < 0.01$, $^{*}p < 0.05$. vs. diabetic control.

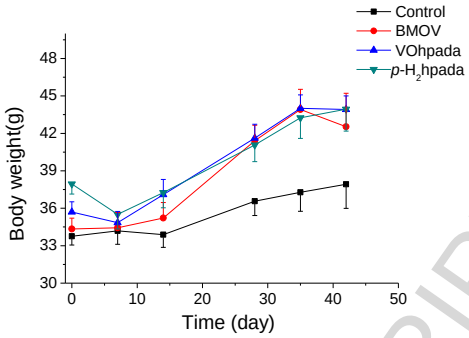

Fig.4 Changes of body weight during treatment with VOphpada. Control diabetic mice (—■—), BMOV-treated diabetic mice (—●—), VOphpada-treated diabetic mice (—▲—), *p*-H_2hpada-treated diabetic mice (—▼—). *n*=7 for each group.

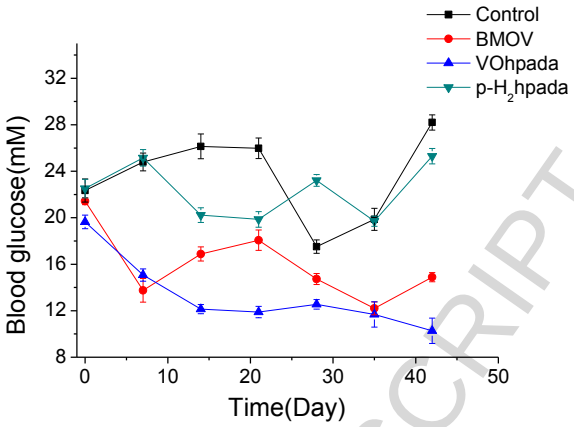

Fig.5 Changes in blood glucose levels upon vanadium treatment. Control diabetic mice(—■—), BMOV-treated diabetic mice (—●—), VOphpada-treated diabetic mice(—▲—) , *p*-H_2hpada-treated diabetic mice(—▼—). *n*=7 for each group.

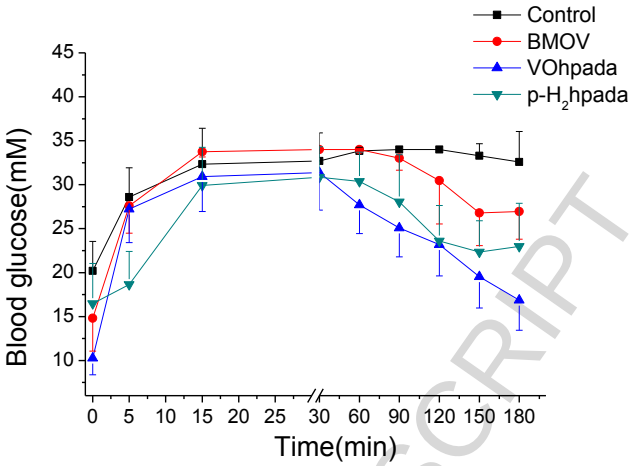

Fig.6 Oral glucose tolerance test curves. Control diabetic mice (—■—), BMOV-treated diabetic mice (—●—), VOphpada-treated diabetic mice (—▲—), ligand-treated diabetic mice(—▼—). *n*=7 for each group.

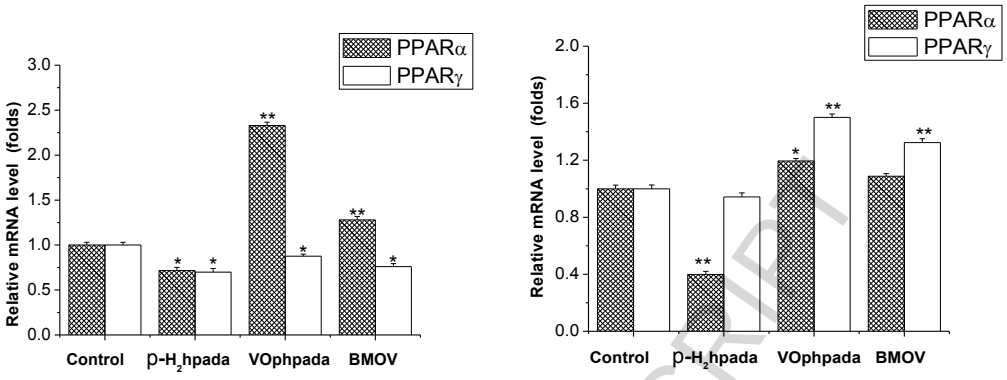

(A) muscle (B) fat

Fig.7 Effects of VOphpada on mRNA levels of PPARα and PPARγ in muscle (A) and fat tissues (B). n=7 for each group. $^{**}p < 0.01$, $^{*}p < 0.05$. vs. diabetic control.

A

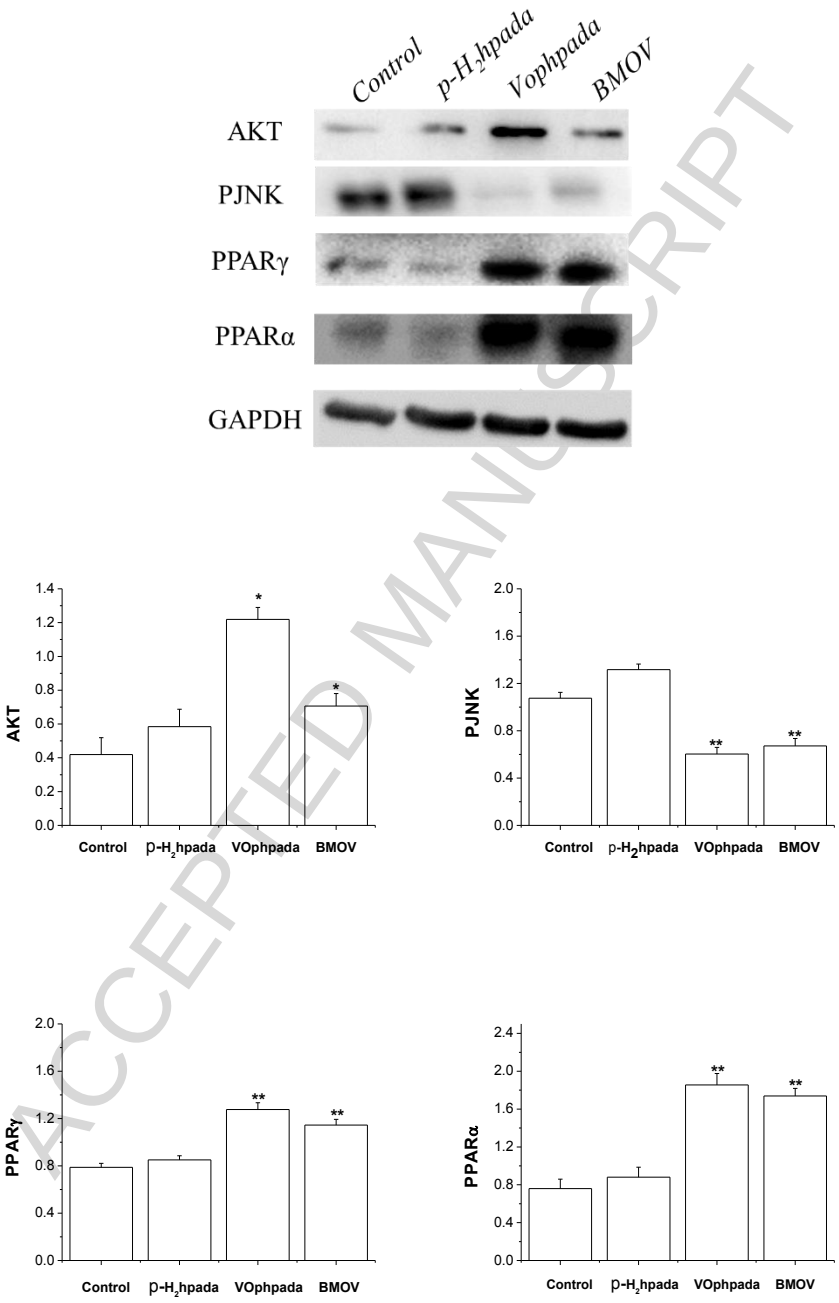

B

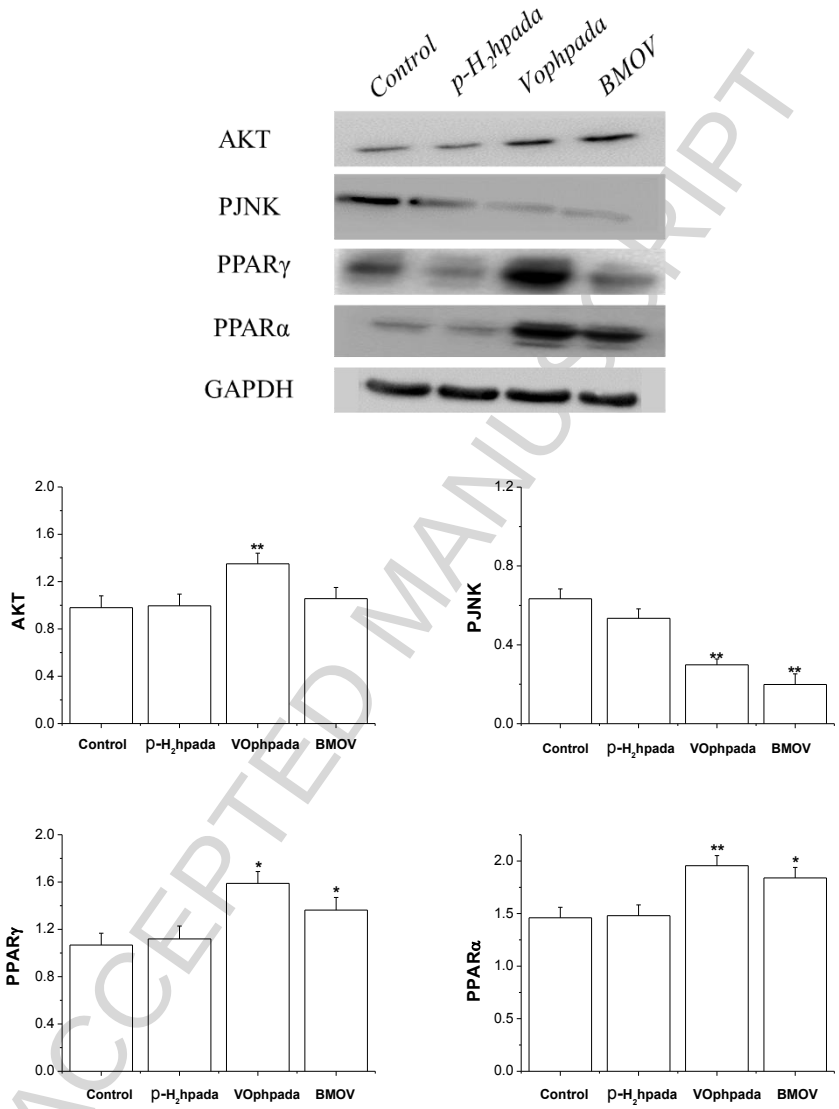

Fig.8 Effects of VOphpada on Akt/PKB, PPARα, PPARγ, and pJNK in muscle (A) and fat (B).

The proteins were extracted and analyzed by western blot as described in the experimental section.

**$p < 0.01$, *$p < 0.05$. vs. diabetic control.

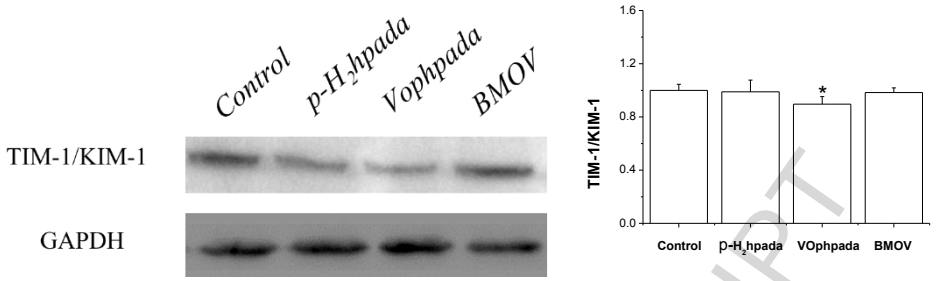

Fig.9 Effects of VOphpada on kidney injury molecule-1 (TIM-1/ KIM-1). The proteins were extracted and analyzed by western blot as described in the experimental section. $^{**}p < 0.01$, $^{*}p < 0.05$. vs. diabetic control.

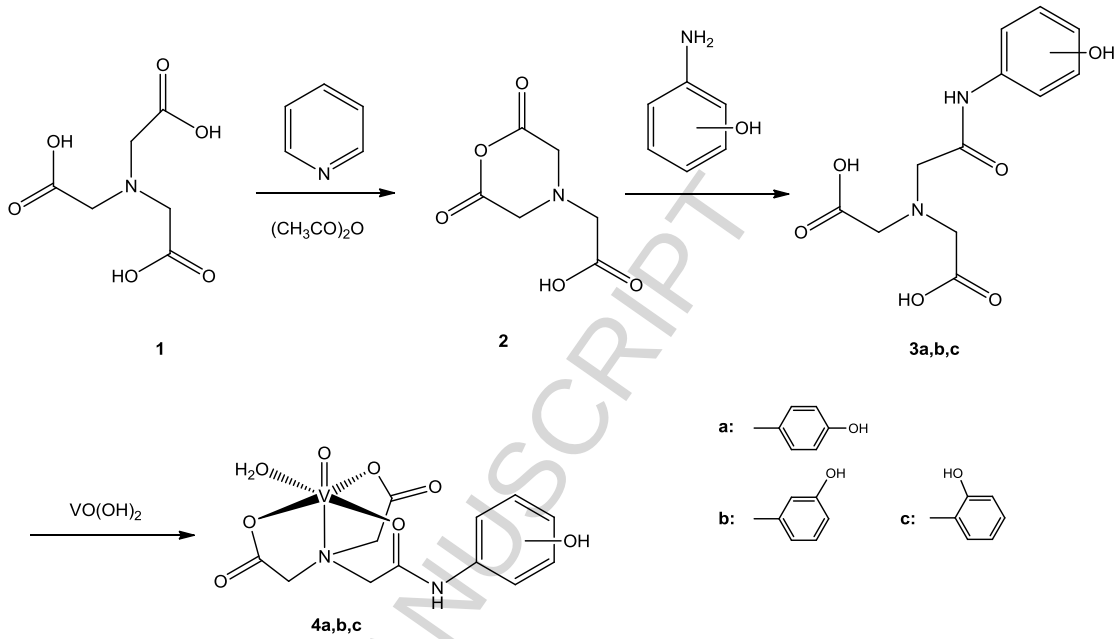

Scheme.1 The synthesis route for vanadyl N-(hydroxyphenylcarbamoylmethyl) iminodiacetate (VOhpada).

Graphical abstract

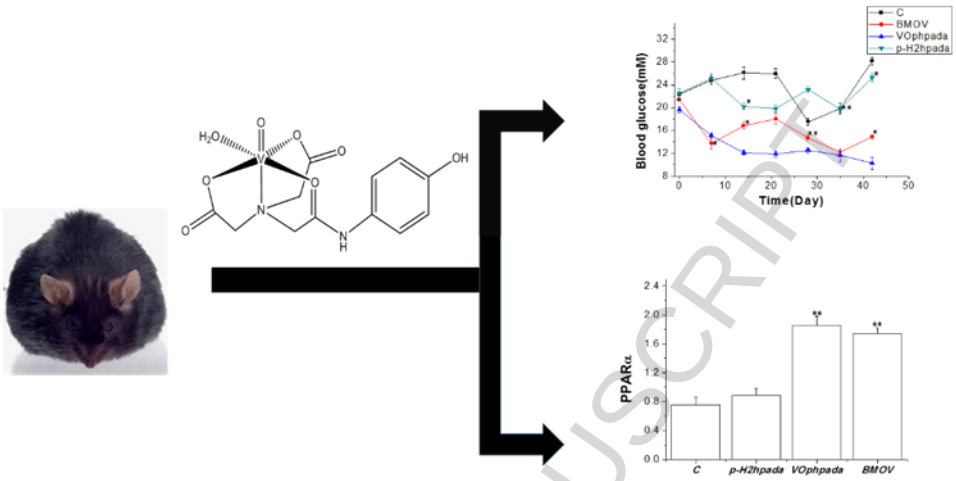

A novel low toxic vanadyl complex (VOphpada) was synthesized by incorporating antioxidant 4-aminophenol in ligand. VOphpada exhibited potent hypoglycemic effects via stimulating insulin enhancement signaling, i.e. increase of PPARα and γ, activation of Akt while inactivation of JNK in muscle and adipose tissues.

Highlghts

- The novel aminophenol-derivatized nitrilotriacetic acid vanadyl complexes (VOphpada) showed more potent insulin enhancement effect than BMOV on type II diabetic *db*/*db* mice and improved index of efficacy over toxicity;
- VOphpada treatment significantly increased expression of PPARα and γ, activated Akt, and inactivated JNK in muscle and adipose tissue. It is the first observation that vanadium compounds could activate PPARα.
- In structure-activity relationship, the position of the hydroxyl group of aminophenol moiety was observed to regulate the antioxidant activity and cytotoxicity of the complexes;
- As candidate drug, VOphpada exhibit better physicochemical properties over BSOV, e.g. reduced molecular size and improve the solubility;